HARD ROCKS AQUIFER PROPERTIES ESTIMATION AND MAPPING THE OPTIMAL DEPTH OF WELLS TO DRILL IN DIVOGUITRY AREA, SOUTHERN CÃ TE DÂ IVOIRE

by Jana Publication & Research

Submission date: 24-Oct-2025 12:23PM (UTC+0300)

Submission ID: 2772508878 **File name:** IJAR-54488.pdf (1.16M)

Word count: 8134 Character count: 39782

HARD ROCKS AQUIFER' PROPERTIES ESTIMATION AND MAPPING THE OPTIMAL DEPTH OF WELLS TO DRILL IN DIVO-GUITRY AREA, SOUTHERN CÔTE D'IVOIRE

Manuscript Info

Manuscript History Received: xxxxxxxxxxxxxxxxx Final Accepted: xxxxxxxxxxxx Published: xxxxxxxxxxxxxxxxx

Key words:

Statistical analysis, conductive fissures, cumulativepercentages discharges, Divo-Guitry.

The nearby study analyses the solid waste management in Tamil Nadu. Solid waste comprised all the wastes arising from human and animal activities that are normally solid and that are discarded useless or unwanted. The increasing difficulty in managing wastes in different states in Tamil Nadu. On the basis of the results, it was recommended to increase public awareness through enlightenment campaign against danger of indiscriminate dumping of wastes as they affect human

Copy Right, IJAR, 2019,. All rights reserved.

27 28 29 Introduction: -

Hard rocks or crystalline rocks (i.e., plutonic and metamorphic rocks) constitute the basement of all continents and are particularly exposed at the surface in the large shields of Africa, India, North and South America, Australia and Europe (Lachassagne et al. 2021). These rocks become aquifers only when they are affected by ruptures (cracks, fractures). The latter concentrates most of the water resources of the to ement aquifers (Tagnon et al., 2018). These aquifers are of strategic importance, particularly in rural areas and regions where surface water resources remain limited. Indeed, although the discharges from these aquifers are relatively modest, they regularly provide drinking water relatively closer to the population and protected from pollution and climatic hazards. However, these aquifers are complex (Kozumé, 1999) and are therefore the subject of numerous studies (Biémi, 1992; Savané, 1997, Kouamé, 1999, L₃₅1, 2000; Holland and Witthüser, 2011; DesRoches et al., 2014; Douagui et al., 2019; Lachassagne et al. 2021; Akpan et al., 2023; Walraevens et al., 2025). This complexity is explained by the fact that, in the hard rocks, the levels of weathering and fracturing are variable. This implies a discontinuous spatial distribution of aquifer's rec 22e, storage capacity and permeability. Thus, it is relatively difficult to predict the flow rates to be extracted from the hard rock aquifers and the path of the water flowing there. Drinking water supply campaigns from boreholes a 19 herefore marked by uncertainties and the failure rates noted there often exceed 70 % (Tagnon et al., 2016, 2018; Courtois et al. 2010; Vouillamoz et al. 2014; Alle et al. 2018). These failures are due to the combination of several factors, including poor knowledge of the complex hydrogeological environment of hard rock aquifers. They represent significant economic losses in investment in drinking water supply projects. For example, currently in Côte d'Ivoire, the average cost per linear meter dug in the hard rock areas can be estimated at 25,000 CFA francs (or £38.11). Thus, if a drinking water supply project drills 100 boreholes, each reaching a depth of 100 m, a failure rate of 40 % will correspond to a loss of 100,000,000 CFA francs (or £152,449.02) on the

.....

Several studies, most of which used a multidisciplinary approach, have advanced the several studies, most of which used a multidisciplinary approach, have advanced the several studies, most of which used a multidisciplinary approach, have advanced the several studies, most of which used a multidisciplinary approach, have advanced the several studies are several studies. rock aguifers. Relatively recent work (Lachassagne et al., 2009, 2011, 2015, 2021; Cho et al., 2002; Wyns et al., 2004; Maréchal et al., 2003; Dewandel et al., 2006, 2011) has widely popularized within the scientific community the concept of "aquifer generated by the weathering process". This work showed that it is the weathering process, not tectonic movements and lithostatic decompression, that is the key factor that transforms hard rock into an envirement capable of containing exploitable groundwater. This work argued that the weathering process begins with the swelling of certain minerals such as biotite. From there, cracking and fracturing begin, the outcome of which is dictated by the evolution of the weathering process at the rock scale. In the weathering profile that develops, the hydrodynamic parameters (transmissivity, sto 23 e) are linked to the lithology and geometry of the different layers constituting the weathering profile (Courtois et al., 2010).

The conceptual model of the hard rock aquifers there 25: suggests a quasi-continuity of hydrodynamic properties, at the scale of a given rock type. This approach makes it personal in the scale of a given rock type. This approach makes it personal is the hydrodynamic properties of these aquifers and gives rise to practical applications such as the sustainable management of water resources at the scale of watersheds, through multi-layer mathematical modeling tools (Lachassagne et al., 2009, 2011, 2015, 2021).

The statistical analysis of borehole data within the concept of aquifer generated by the weathering process, as developed by Courtois et al. (2010), is of great interest, particularly in rural areas of developing countries. In these countries, adequate funding for multidisciplinary hydrogeological exploration and water well drilling is often unavailable, especially in rural areas. Thus, for localities where a database of previously drilled boreholes and regional geological maps exist, statistical processing of borehole data, from the perspective of the aquifer concept generated by the deep rock weathering process, provides valuable information could guide future drilling campaigns and be taken into account in the implementation of sustainable water resource management tools.

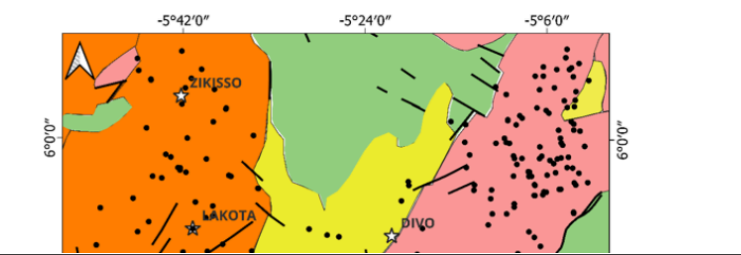
This study, which is applied to the Divo-Guitry area, statistically processes the process relative process. Like the entire southern forest part of Côte d'Ivoire, Divo-Guitry is a strategic area in the Ivorian economy. Indeed, with a dense population, Divo-Guitry is high agricultural production area, with, in addition, rapidly expanding mining activities. The pressure of these activities on water resources is increasing. All of this appears to be exacerbated by the effects of climate change. This area needs to address its syming water needs and develop a sustainable water resource management tool (Tagnon et al., 2016, 2018, 2020). The objective of the study is to assess the geometric and hydrodynamic properties of the Divo-Guitry fractured hard rock aquifer to guide the location of fute water wells. It identifies the specific hydrogeological parameters associated with each rock type, determines the most productive zones in the fractured layer, the average productivity of the aquifer, and estables a spatial distribution of optimal well depths to drill. This work is a continuation of previous ones as sensing et al., 2014; Kouamé et al., 2021; Aoulou et al., 2021; Bouatrin et al., 2022) conducted in different areas of Côte d'Ivoire and which adopted the same approach to statistically analysis drilling data. However, this study is notable for its statistical analysis, distinguishing three types of crystalline rocks (metatonalite, metagranite, and metagranodiorite) and providing a map of the optimal drilling depth.

The information obtained will be 24 important contribution to hydrogeological exploration and the development of a water resource management tool at the regional scale.

2. Methodology

2.1. Study area

 Divo-Guitry area is in the southern part of Côte d'Ivoire, between longitudes 5 ° and 6 ° West and latitudes 5°27' and 6 °10' East (Figure I).



71	
72	
73	
74	
75	
76	
77	
78	
79	
00	
80	A Y
81	
82	
92	
83	
84	
85	
86	
80	34
87	Figure 1. Map presenting the study area and distribution of lithological formations
88	This area covers 144 km² and includes the localities of Zikisso, Lakota, Divo, Guitry, and Gbagbam. It is an area of
89	dense and fast-growing population (over 3.8 % / year), pacticing intense agricultural activities and where mining
90	operations are expanding rapidly (Tagnon et al., 2020). The climate consists of 4 seasons: long dry season from
91 92	November to February; long rainy season from March to June; short dry season between July and August and
12	finally, short rainy season from September to October.
93	Geomorphologically, the landscape is relatively flat, with elevation decreasing from 300 m above sea level (ASL) in
94	the North-west (in Zikisso area), to 20 m ASL in the South-east (in Guitry area). Thus, following the arrangements
95	of the geological formation bands, the thicknesses of the saprolites are generally greater on the biotite metagranite
96	(MGR) than on the biotite metagranodiorite (MGDR), where they are also higher than on the metatonalite (MTR)
97	(Tagnon, 2021).
98	The information about geology of the study area is mainly extracted from Delor et al. (1995). The geological
99	formations belong to Paleoproterozoic (Geomines 1982; Delor et al., 1995) and consist of volcano-sedimentary
00	rocks and intrusive rocks.
.00	
01	Volcano-sedi variatively small in extent across the study area. Two blocks, one in the northern part

- Intrusive rocks essentially cover the study area. These rocks consist of biotite metagranite (M31), biotite and/or hornblende metagranodiorite (MGDR), and metatonalite (MTR). The MGR below xtends across the western part of the study area and includes the localities of Zikisso and Lakota. The MGDR is in the central part of the study area and borders the northern block of volcano-sedimentary rocks. The MTR belt, elongated NE-SW, exter(1) between the MGDR and the northern block of volcano-sedimentary rocks on the one hand, and the eastern block of volcano-
- 109 2.2. Data

- 110 Digital geological maps and data from water boreholes pre used for this study. The geological maps are from the
- square degrees of Grand-Lahou and Gagnoa and were provided by the geology department of Côte d'Ivoire. The
- 112 water wells are distributed upon three types of lithology which are MGR, MGDR and MTR.
- The database contains 275 borholes, distributed across geological formations as follows: 33 on MGDR, 92 on MGR
- and 150 on MTR. Each borehole in the database is informed with the following informations: X, Y, and Z
- 115 2 ordinates; geology; total depth; saprolite thickness; depth to static level; depth and fdischarfes of inflows and
- instantaneous discharge (air lift flow measured at the bottom) end of the drilling by blowing air under pressure at the bottom
- 117 of the well (Courtois et al., 2010)). All boreholes cross the saprolite horizon and capture the fissured layer.
- 118 2.3. Methods
- 119 The work consisted of analyzing data from boreholes dug on three types of intrusive geological formations: MGR,
- 120 MGDR and MTR. The study was carried out on these three types of lithologies because they cover almost the entire
- study area and the data we have there has a heterogeneous distribution.
- 122 First, a statistical analysis was performed to determine the distribution of each borehole parameter. Next, the
- 123 analysis focused on the variation of aquifer properties with depth. Finally, the optimal total depth of borehole to drill
- 124 was estimated, and a map highlighting the spatial distribution of this total depth was created.
 - 2.3.1. Elementary Statistical Analysis

sedimentary rocks on the other (Figure 1).

- 126 De borehole parameters analyzed are: Total depth of borehole (Td); Saprol thickness (St); Length of borehole
- below the base of saprolite (Lbs) and Instantaneous discharge (Qi) (air-lift flow rate at the end of development).
- 128 Each parameter, which is in fact a statistical variable, was classified into classes and the frequency of each class was
- 129 calculated. A comparative analysis of the parameter frequencies, based on lithology, was then performed.

130 131

125

132 2.3.2. Analysis of the vertical varia

2.3.2. Analysis of the vertical variation of aquifer properties

- 133 The geometric and hydrodynamic properties of the aquifer were highlighted. The analysis first focused on the
- distribution of inflows, according to the length of borehole below the base of the saprolites (Lbs).
- 135 Inflows are assumed to be associated with conductive fissure zones. Analyzing the distribution of inflows it depth
- 136 could provide insights into the permeable zones of the aquifer. Secondly, the distribution of the cumulative
- 137 percentage of linear discharges, as a function of the length below the base of the saprolites (Lbs), was studied. This
- 138 step gave rise to the concepts of linear discharges, cumulative percentage of linear discharges, and average aquifer
- 139 productivity.
- 140 2.3.2.1. Linear discharge

- 141 Linear discharge represents the instantaneous discharge per meter of rock formation cross d. For the study of aquifer
- properties, the linear discharge was preferred to the instantaneous one. The latter could be a biased variable because
- it can depend on the total depth of the well (Courtois et al., 2010). Indeed, the total depth of the well would be an
- arbitrary value, depending more on obtaining an adequate or desired discharge. This value therefore cannot reflect
- 145 the intrinsic properties of the aquifer.
- Linear discharge can be a function of the total depth the well or can be defined ative to the length of well below
- the base of the saprolites. In this study, linear discharges were estimated relative to the well length below the base of
- 148 the saprolites, using the expression:

$$q_i(l_i) = \frac{Q_i}{l_i}, i = 1, n \tag{1}$$

- 149 Where
- 150 Qiis the instantaneous discharge;
- 151 li is the length from the base of the saprolites;
- 152 qirepresents the linear discharge, referring to the length below the base of the saprolites;
- i is the rank of the well;
- n is the total number of wells.
- 155 2.3.2.2. Cumulative percentage of linear discharge
- 156 The cumulative percentage of linear discharge is highlighted through the following relation:

$$P_q(L) = \sum_{l=Lmin}^{l=L} qi(l) / \sum_{l=Lmin}^{l=Lmax} qi(l)$$
(2)

- 157 Where
- 158 P_q(L), denotes the cumulative percentage of linear discharge, whose length below the base of the saprolites is less
- 159 than L (m)
- 160 Each linear discharge corresponds to a value of well length below the base of the saprolites L (m). The linear
- 161 discharges are ranked according to increasing values of L (m). The cumulative percentages of linear discharges
- 162 $(P_q(L))$ therefore vary from $P_q(Lmin) = 0$ %to $P_q(Lmax) = 100$ %.
- The curve linking each $P_q(L)$ to the corresponding well length below the base of the saprolites is produced (Figure
- 3). Analysis of this curve 7 ghlights the most transmissive zone of the aquifer. The latter is obtain through the
- portion of the curve that presents a linear trend and corresponds to the "Useful Thickness (Lu)" of the aquifer
- 166 (Courtois et *al.*, 2010) (Figure 2).

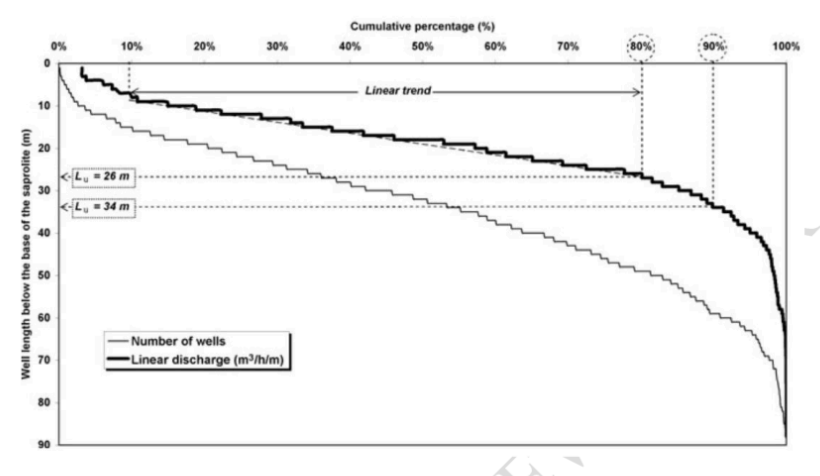


Figure 2: Curve of cumulative percentages of linear discharges for estimating aquifer fissured layer properties (after Courtois et al., 2010)

170 2.3.2.3. Average aquifer productivity

167

171 The average productivity relative to the Lu is determined according to the relations:

$$q_M(Lu) = \sum_{l=Min(ll,i=1,n)}^{Lu} q_i(l)/j(Lu), \qquad i = 1, n$$
(3)

$$Q_M(Lu) = q_M(Lu) \times Lu \tag{4}$$

- 173 L_U is the effective thickness of the fissured zone;
- 174 $q_M(Lu)$ is the average linear discharge, obtained with Lu;
- 175 j(Lu) is the number of wells corresponding to Lu;
- 176 $Q_M(Lu)$ denotes the average discharge obtained with the Lu.
- 177 $Q_M(Lu)$ is the resulting mean discharge for theoretical wells that would intersect the whole useful thickness (Lu)
- of the fissured layer (Courtois et al., 2010).

179 **2.3.3.** Estimating the Optimal Drilling Depth

- 180 We define the optimal drilling depth as the depth that must be reached when drilling the borehole to ensure that the
- entire most transmissive zone of the aquifer is captured. The areabeyond the optimal depth is a contingency zone.
- 182 The driller may encounter a conductive or non-conductive fracture there, and the risk of financial losses on the
- 183 investment cost is higher.

184 At a given point, the optimal depth (Pop) corresponds to the useful length (Lu) increased by the thickness of the saprolites.

$$P_{op} = Lu + St (5)$$

186 To make Pop an integer, each value of Lu and St, which is a decimal number, was rounded up to the nearest whole number.

The kriging method was used to create a map showing the spatial distribution of the optimal drilling depth.

189 3. Results and discussion

190 **3.1. Results**

191

3.1.1. Statistical distribution of well parameters

The results of the statistical study of borehole parameters are presented in Table 1 below.

193 Table 1: Statistical distribution of borehole parameter frequencies according to classes

Total depth of borehole (m)					
				100 100	
3 (mp	25 -50	50 -75	75 -100	100 -120	
MTR	38.42	44.63	15.81	1.13	
Frequency (%)					
MGR	13.04	61.96	25	0	
Frequency (%)					
MGDR	38.24	44.12	17.65	0	
Frequency (%)					
		Thickness of the sa			
	0 - 25	25 -50	50 -75	75 - 85	
MTR	80	20	0	0	
Frequency (%)		()			
MGR	40.22	55.43	4.35	0	
Frequency (%)					
MGDR	58.82	41.15	0	0	
Frequency (%)	14				
Length of borehole below the base of saprolite (m)					
	0 – 35	35 -65	65 -95	95 – 125	
MTR	35.80	50.57	13.07	0.57	
Frequency (%)	/				
MGR	49.45	42.86	7.61	0	
Frequency (%)					
MGDR	50	44.12	5.88	0	
Frequency (%)					
Instantaneousdischarge (m³/h)					
	0 - 2,5	2,5 - 5	5 – 10	10 – 20	
MTR	50	22.08	19.48	8.44	
Frequency (%)					
MGR	69.32	11.36	13.64	5.68	
Frequency (%)					
MGDR	57.14	25	10.71	7.14	
Frequency (%)					

1	9	4
1	9	5

3.1.1.1. Total depth of boreholes (TD)

- 196 All the boreholes in the database, carried out on each of the lithologies, have total depths (TDs) between 30 and 115
- 197 m. The interval 50 to 75 m has the highest frequencies, while the frequencies are almost zero on the interval 100 to
- 198 $\,$ $\,$ 120 m, whatever the lithology. The TDs, between 50 and 75 m, represent 44.63 %, 61.96 % and 44.12 %,
- respectively, on the MTR, MGR and MGDR. Following this same order of lithologies, the frequencies are 38.42 %,
- 200 13.04 % and 38.24 %, for the TDs vary between 25 and 50 m. Boreholes with TDs ranging from 50 to 100 m have
- frequency estimates of 60.44 %, 86.96 %, and 61.77 %, on the MTR, MGR, and MGDR rocks, respectively.
- 202 Overall, the highest TDs are most frequently encountered first on the MGR, then on the MGDR, and then on the
- 203 MTR.

204 3.1.1.2. Thickness of the saprolite (TS)

- 205 Saprolite thickness range from 1.28 to 48.65 m on the MTR, from 3.08 to 72.05 m on the MGR and from 7.54 to
- 206 48.59 m on the MGDR. Boreholes with saprolite thicknesses less than 25 m represent 80 % on the MTR band, while
- 207 on the MGR and MGDR they occupy 40.22 % and 58.82 % respectively. Saprolite thicknesses between 25 and 50 m
- 208 occupy 20 %, 55.43 % and 41.15 % respectively on the MTR, MGR and MGDR. Beyond 50 m, the frequencies are
- zero, except on the MGR, where the frequency is 4.35%.
- 210 The lowest saprolite thicknesses (≤ 25 m) have a greater occurrence on the MTR, then on MGDR and then on MGR.
- 3.1.1.3. Length of borehole below the base of saprolite (Lbs)
- Length of boreholes below the base of saprolite (Lbs) less than 35 m represent 35.80 %, 49.45 %, and 50 %,
- 213 respectively, for the MTR, MGR, and MGDR rocks. In the same order, Lbs between 35 and 65 m represent 50.57 %,
- 214 42.86 %, and 44.12 %. Between 65 and 95 m, the frequencies are 13.07 %, 7.61 %, and 15.88 %, respectively. There
- 215 are virtually no Lbs exceeding 95 m.
- 216 The longest Lbs are slightly more common in the MTR than in the other two lithologies (MGR and MGDR). The
- 217 frequencies of the Lbs classes, on the latter two (MGR and MGDR) are significantly close.

218 3.1.1.4. Instantaneous discharges (Qi)

- 219 Instantaneous discharges (Qi) below 20 m³/h are statistically analyzed. On the MTR, eight (8) Qi values, including
- 220 one of $45 \text{ m}^3/\text{h}$, are above $20 \text{ m}^3/\text{h}$. Five (5) Qi values above $20 \text{ m}^3/\text{h}$ are noted, including one reaching $90 \text{ m}^3/\text{h}$, on
- the MGDR. Finally, on the MGR, only one (1) Qi value (21.6 m³/h) is above 20 m³/h.
- Low Qi (2.5 m³/h) are more common. Their frequencies are 50 %, 69.32 %, and 57.14 %, respectively, on the MTR,
- MGR, and MGDR. These Qi are most frequently observed on the MGR (69.32 %), while the MTR recorded the
- lowest frequency (50 %). On the other hand, regarding average Qi (2.5 m 3 /h < Qi <5 m 3 /h), the highest frequency is
- 225 noted on the MGDR (25 %) and the lowest is obtained on the MGR (11.36 m³/h). Qi values below 5 m³/h represent
- 226 72.08 %, 80.68 % and 82.14 %, respectively, on the MTR, MGR and MGDR.
- 227 Overall, we note that the highest Qi have a relatively higher occurrence on the MTR and lower occurrence on the
- 228 MGR.

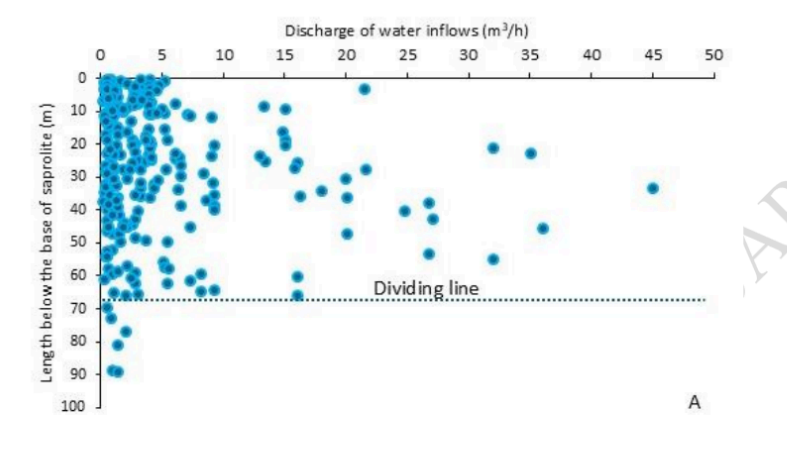
229 3.1.2. Properties of the Divo-Guitry hard rock aquifer

230 3.1.2.1. Vertical distribution of inflows and cumulative percentages of linear discharges

233	of the saprolites, in the case of MTR, are illustrated in Figure 3.
234	Inflows are observed between 0 and 90 m below the base of the saprolites (Figure 3a). However, these tend to
235	decrease with depth. This decrease with depth appears more marked after 50 m, and even more so, from 68 m,
236	below the base of the saprolites (see the dividing line in Figure 3a). The discharges associated with these water
237	inflows are mostly (75.30 %) less that makes with associated discharges greater than 5 m³/h (the most
238	variable flow rates) are predominant between 10 and 68 m below the base of the saprolites. There are several
239	significant discharges between 15 and 35 m ³ /h and one of 45 m ³ /h. This zone between 10 and 68 m is the zone
240	where the flow rates are the most variable ($> 5 \text{ m}^3/\text{h}$).
	4
241	The curve of the variation of the cumulative percentages of linear discharges as a function of the length below the
242	base of the saprolites is presented in Figure 3b. This curve starts with 0 %, around 10 m. For its interpretation, it can
243	be split into three parts:
244	• the first part is between 0 and 4 %, with relatively steep slope, which would reflect two hypothes either a low
245	density of conductive fissures, in the first meters below the base of the saprolites, or an uncertainty in the location of
246	the saprolite-fissured zone interface; this second hypothesis seems the most plausible;
247	\bullet the curve adopts a gentle decrease, highlighted by the somewhat linear shape it follows, down to 88 % (or even a
248	little more), corresponding to 53.99 m, representing the useful length (Lu); this suggests a regular decrease in linear
249	discharges, which would mean that the number of conductive fissures would be steadily decreasing with depth; this
250	zone would contain the most variable instantaneous discharges and would be the most productive zone of the
251	aquifer;
252	• after the quasi-linear zone, the graph curves and thus seems to mark the rapid decrease in linear dispharges with
253	depth; this part of the aquifer would correspond to the lowest part of the fissured zone and would be characterized
254	by a low density of conductive fissures.
255	
	O Y
	X Y

The distributions of inflows and cumulative percentages of linear discharges, as a function of length below the base

a) Metatonalite Rock (MTR)



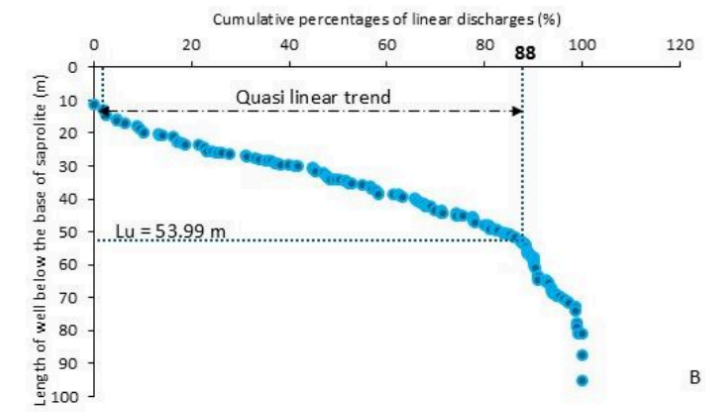


Figure 3. Vertical distribution of the properties of the MTR aquifer: a) analysis with inflows; b) analysis with cumulative percentages.

The useful length (Lu) of 53.99 m (obtained at 88 %), below the base of the saprolites, appears to contain the highest density of conductive fissures. This Lu could be considered the horizon of the fissured layer, above the unweathered MTR.

To ensure optimum productivity, we suggest that boreholes drilled on the MTR necessarily reach 53.99 m below the base of the saprolites.

The average discharge obtained at this optimum depth of 53.99 m is $7.0 \text{ m}^3/\text{h}$.

b) Biotite metagranite rock (MGR)

The distributions of inflow discharges and cumulative percentages of linear discharges, as a function of length below the base of the saprolites, for MGR, are presented in Figures 4a and 4b, respectively.

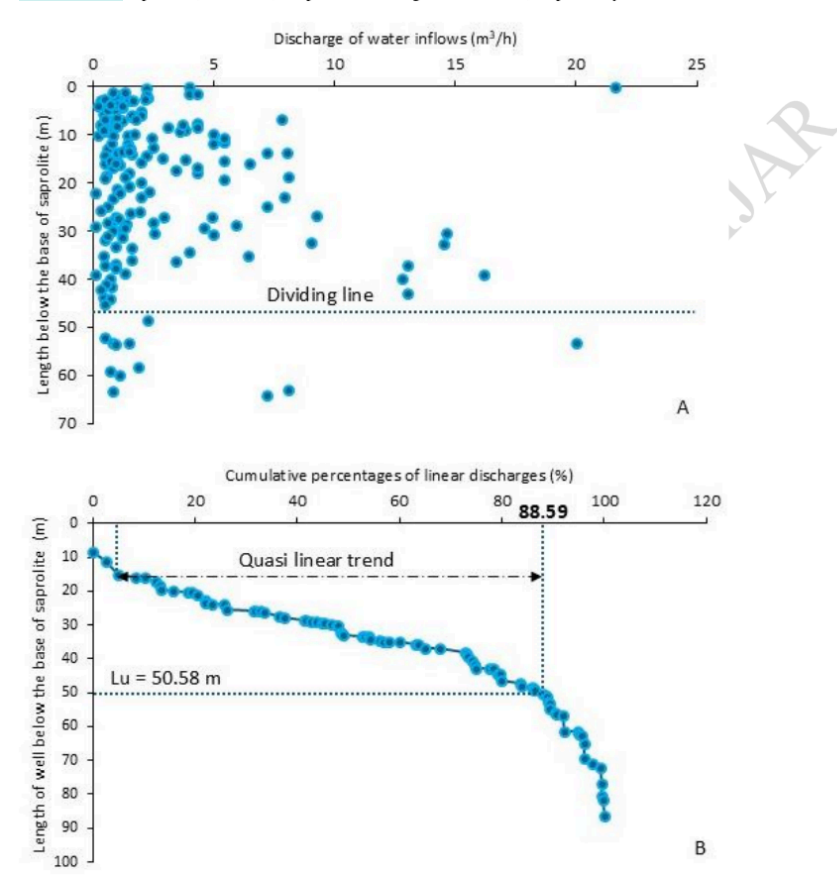
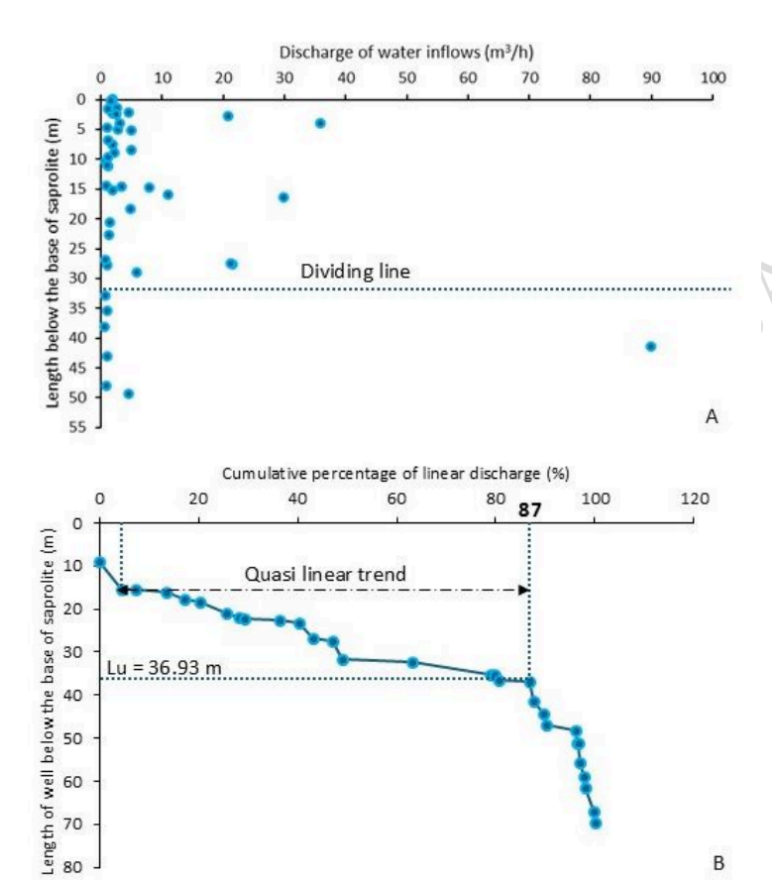


Figure 4. Vertical distribution of the properties of the MGR aquifer: a) analysis with water inflows; b) analysis with cumulative percentages.

Inflows are present between 0 and 65 m below the base of the saprolites (15 ure 4a). However, their occurrence appears to decrease with depth. This is particularly noticeable after 46 to 47 m, below the base of the saprolites (see the demarcation line in Figure 4a). Most of the inflow discharges (83.43 %) are less than 5 m³/h. An exceptional discharge of 21.6 m³/h is observed at the saprolite-fissured zone interface (0 m). The inflow discharges are more

- 275 variable between 10 and 46 m. Beyond 46 m, there are 3 boreholes with inflow discharges greater than 5 m³/h,
- 276 including one value reaching 20 m3/h.
- The curve showing the evolution of cumulative percentages of linear discharges as a function of length below the 277
- 278 base of the saprolites shows a regular decrease (Figure 4b). It also highlights the three parts described above, in the
- 279 case of the MTR. The first rt, between approximately 0 and 5 %, with a relatively steep slope, certainly reflects
- 280 the effect of uncertainty in the location of the saprolite-fissured zone interface. The second part takes on a quasi-281
- linear appearance up to 88.59 %, corresponding to 50.58 m, before carrying. This suggests the regular decrease with depth of conductive fissures and that these are denser in the first 50 meters below the base of the saprolites. When 282
- 283 drilling a borehole on MGR, reaching a depth of 50.58 m, below the base of the saprolites, which corresponds to the
- 284 useful length (Lu), could ensure optimal exploitation of the aquifer.
- 285 The average flow rate obtained with the useful length (Lu) of 50.58 m is 5.14 m³/h.
- c) Biotite metagranodiorite rock (MGDR) 286
- Figures 5a and 5b show, respectively, the distributions of inflow discharges and the cumulative percentages of linear 287
- 288 discharges, as a function of length from the base of the saprolites, in the case of MGDR.
- 289 The number of inflows decreases with depth, and this appears more pronounced after 30 m (see demarcation line in
- 290 Figure 5a), below the base of the saprolites (Figure 5a). 75 % of the water inflow rates are less than 5 m³/h. The
- most variable discharges are in the first 30 meters, below the base of the saprolites. However, significant discharges 291
- 292 can be encountered beyond these 30 m. In fact, an exceptional discharge of 90 m³/h is highlighted, around 40 m,
- 293 below the base of the saprolites.
- Like the other curves (Figures 3b and 4b), the curve in Figure 5b decreases and mainly shows three parts. The first 294
- 295 part starts from 0 to about 4 %, with a relating steeper slope. Asmentioned above (see the analysis on the MTR),
- 296 this steep slope could mean an uncertainty related to the positioning of the saprolite-fissured zone interface. The
- 297 second part (quasi-linear part) extends between 4 and 87 % and highlights the greatest density acconductive fissures
- 298 in the aquifer. This zone corresponds to the useful length (Lu) which is estimated at 36.93 m, below the base of the
- 299 saprolites. Within the quasi-linear zone, points indicating slope breaks (40.13% and 47.07%), which are relatively
- 300 less significant, are perceptible. Finally, the third part, which is located beyond 87 % (36.93 m), characterized by a
- 301 steep slope, indicates the lowest part of the fissured zone, resulting from its low density of conductive fissures. To
- sure optimum productivity, it would be desirable for boreholes drilled on MGDR to necessarily reach 36.93 m 302
- 303 below the base of the saprolites.
- 304 The average flow rate obtained with the Lu of 36.93 m is 8.30 m³/h.



 $Figure \ 5. \ Vertical \ distribution \ of \ the \ properties \ of \ the \ MGDR \ aquifer; \ a) \ analysis \ with \ inflows; \ b) \ analysis \ with \ cumulative \ percentages$

${\bf 3.1.3.\,Spatial\,\,distribution\,\,of\,\,optimal\,\,drilling\,\,depth}$

Optimal drilling depths range from 45 to $124 \, \text{m}$. Figure 6 below highlights the spatial distribution of optimal drilling depths. The greatest values (from 89 to $100 \, \text{m}$, or even more) are observed along the MGR belt, particularly between Gagnoa and Zikisso, and extend towards Lakota. Intermediate depths (67 to $88 \, \text{m}$) are also more spread out across the MGR.

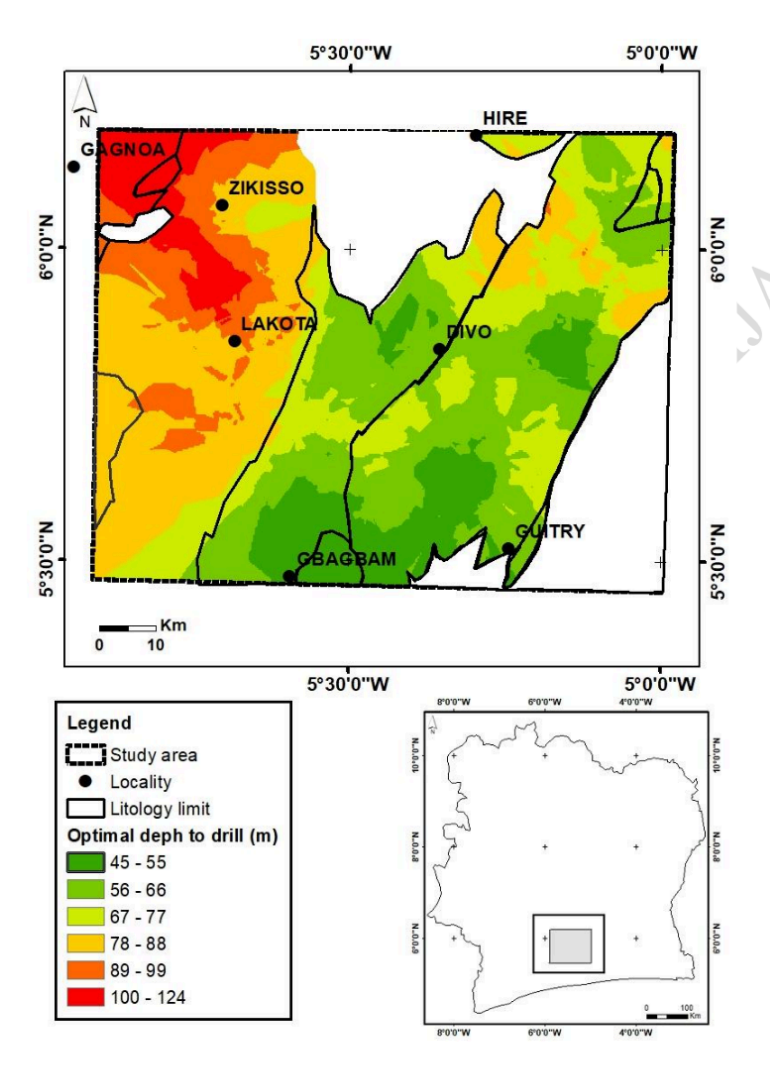


Figure 6. Spatial distribution of optimal drilling depths

 These depths, ranging from 67 to 88 m, are noted on the MGDR and MTR belts, particularly in the northeastern part. The shallowest depths (45 to 66 m) are observed on the MGDR and MTR.

- In the southern part, around Gbagbam and between Gbagbam and Guitry, the shallowest optimal depths (45 to 55 m)
- 320 are present. They also extend towards Divo.
- 321 Overall, the spatial distribution of optimal drilling depths is guided by the spatial distribution of saprolite
- 322 thicknesses.

3.2. Discussion

- The borehole parameter values were divided into different classes, and the class sizes were subject to a comparative 324
- 325 analysis, based on the geological formations. This study revealed the following:
- 326 - the greatest values of total borehole depths and saprolite thickness are more prevalent first on the MGR, then on
- 327 the MGDR, and finally on the MTR;
- the greatest lengths of boreholes below the base of saprolite are slightly more prevalent on the MTR than on the 328
- other two lithologies (MGR and MGDR), which indicate substantially similar frequencies; 329
- 330 - the discharges range across the three lithologies is dominated by low discharges (< 2.5 m³/h); the highest flow rate
- 331 values are more prevalent, first on the MTR, then on the MGDR, and finally on the MGR.
- These observations would be characteristic of exploitation boreholes, carried out in the middle of the hard rocks of 332
- 333 rural areas. Indeed, the cost of boreholes is determined by the mear meters dug. Also, the total depth of the
- 334 borehole, which includes the thickness of the saprolites and the length by the base of saprolites, is linked to
- achieving a high flow rate or the desired flow rate. Thus, for cost reasons, drilling is most often stopped as soon as 335
- 336 the adequate flow rate is achieved. Flow rates 16 the middle of the hard rock are relatively modest and are generally
- 337
- sufficient for rural areas, where water needs are relatively lower. In the study area, the thickness of the saprolites,
- 338 which are greater in the western part, in the localities of Zikisso and Lakota, decreases steadily towards the east
- 339 (Géomines, 1982). Thus, depending on the arrangement of the geological formations, the order of decreasing
- importance of the thicknesses of the saprolites is as follows: MGR, MGDR and MTR (Tagnon, 2021). 340
- 341 This would explain the results obtained in this study and recalled above, in this section 3.2. Indeed, where the
- 342 thickness of the saprolites is significant (MGR), there is a tendency to have large values of total borehole depth and
- 343 where the thickness of the saprolites is small (MTR), the greatest lengths of borehole below the base of saprolites
- 344 are frequent. Also, in these areasof small thicknesses of the saprolites (MTR), high flow rates also have a greater
- 345 occurrence, certainly because the drillings extend over large lengths below the base of saprolites, thus capturing a
- 346 relatively greater number of conductive fissures.
- 347 The analysis of the distributions of inflows and the cumulative percentages of linear discharges made it possible to
- 348 highlight the geometric and hydrodynamic properties of the Divo-Guitry hard rock aquifer. These two approaches
- 349 revealed similar information for some and complementary information for others. In terms of complementary
- 350 information, we note a decrease with depth in the density of conductive fissures. This was highlighted by the 351
- decrease as a function of depth, in the number of inflows, on the one hand, and the decrease as a function of depth, 352
- in the cumulative percentages of linear discharges, on the order hand. Also, these two approaches revealed, in an 353 almost similar way, for each lithology, the area of greatest density of conductive fissures, under the base of the
- 354 saprolites. In the case of the MGR, this zone was identified at 47 m, below the base of the saprolites, with the
- 355 approach involving inflows and at 50.58 m, with the approach of cumulative percentages of linear discharges. 356 Regarding the complementarity aspect 1 the results, the approach which involves inflows made it possible to note
- 357 the presence of the latter from from first meters below the base of the saprolites. This means that conductive fissures
- 358 would be present from the first meters below the base of the saprolites. This result is not perceptible with the result is not perceptible with the result is not perceptible with the result is not perceptible.
- 359 using the cumulative percentages of linear discharges. Indeed, this method, in its execution, uses the lengths below
- 360 the base of the saprolites, reached by the boreholes. In the database, the minimum values taken by the latter are

around 10 m. This is the reaso the the curves involving the cumulative percentages of linear discharges (Figures 3b, 4b and 5b), start around 10 m, below the base the saprolites. They therefore do not provide information on the presence or not of conductive fissures in the first meters below the base of the saprolites. The complementarity and similarity 43 the information obtained with the two approaches justify their concomitant use in highlighting the geometric and hydrodynamic properties of fractured basement aquifers.

The approaches developed in this study to characterize the properties of the Divo-Guitry aquifer showed a decrease the density of conductive fissures with depth. This observation was also made by sever 17 uthors including Courtois et al. (2010), in Burkina Faso, Aoulou et al. (2021), Kouamé et al. (2021) and Bouatrin et al. (2022), in Côte d'Ivoire. The useful lengths (Lu) obtained are 53.99 m, 50.58 m and 36.93 m, respectively on the MTR, MGR and MGDR. Lu on the MTR and Lu on the MGR are practically in the same order. However, the Lu on the MTR is greater, by about 4 m, than the Lu on the MGR. This difference would be because thegreatest basement lengths reached by the boreholes are more numerous on the MTR than on the MGR. The useful length (Lu) obtained on the MGDR (36.93 m) is relatively lower. However, the average flow rate corresponding to this useful length, which is estimated at 8.30 m³/h, is greater than the average flow rates noted on the other two lithologies (7 m³/h for the MTR and 5.14 m³/h for the MGR). These results would be linked to the particularities of the weathered process on the

Also, it should be noted that the number of b 15 holes used for processing on the MGDR is relatively low. This could introduce biases into the results obtained. In western Côte d'Ivoire, Aoulou et al. (2021) obtained a Lu equal to 43 m, on biotite granodiorites and biotite metagranodiorites. The difference with our study is that our analysis only takes place on the biotite metagranodiorite (MGDR) lithology. Kouamé et al. (2021) obtained a Lu of 40 m, in the Tchologo region and Bouatrin et al. (2022) noted an average Lu of 45 m, in the Marahoué watershed. The results obtained by these authors concern a set of crystalline lithologies. On the contrary, each Lu that we obtained in our study concerns a single lithology. In Burkina Faso, Courtois et al. (2010) noted that conductive fissures have an optimal density between 8 and 25 m below the base of saprolites, on porphyritic biotite granites. The extent of conductive fissures is small compared to those observed in our study. This difference would be related to the local

particularities of the weathering process, which would be deeper in the relatively more humid areas of Côte d'Ivoire.

Beyond the demarcation line highlighted in Figures 3a, 4a and 5a, the presence of inflows in the boreholes is noted.

In some cases, the discharges of these inflows are considerable. This suggests that when drilling beyond the demarcation line or beyond the useful length (Lu), it is possible to encounter open and hydraulically active fractures, which could provide significant, even exceptional, discharges. However, the probability of encountering these hydraulically active fractures is reduced beyond the demarcation line or the useful length (Lu).

Conclusion

 Statistical analysis of drilling parameters revealed that these are characteristics of exploitation boreholes in hard rock zones, particularly in rural areas. Indeed, high total depth values are more common in areas with the greatest saprolite thicknesses, while drilled bedrock thicknesses are relatively greater in areas with thin saprolite thicknesses. Also, the lowest flow rates (2.5 m³/h) are the most frequent. Analysis of geometric and hydrodynamic properties showed that inflows are present from the first few meters below the base of the saprolites and that the density of conductive fissures decreases with depth. The most variable inflow discharges (> 5 m³/h) are noted between 10 and 68 m, 10 and 46 m and at 30 m, under the base of the saprolites, respectively, on the MTR, MGR and MGDR. Following this same order, the calculated useful lengths (Lu), are respectively for m³/h, 5.14 m³/h and 8.30 m³/h.

- 404 References
- 405 1. Akpan A.E., Ekwok S.E., Ben U.C., Ebong E.D., Thomas J.E., Ekanem A.M., George N.J. Abdelrahman K.,
- 406 Fnais M.S., Eldosouky A.M., Andráš P., Alarifi S. S. (2023). Direct detection of groundwater accumulation zones in
- 407 saprock aquifers in tectono-thermal environments. Water. 15, 3946. https://doi.org/10.3390/w15223946
- 408 2. Alle C., Descloitres M., Vouillamoz J. M., Yalo N., Lawson F.M.A., Adihou C. (2018). Why 1D electrical
- 409 resistivity techniques can result in inaccurate siting of boreholes in hard rock aquifers and why electrical resistivity
- 410 tomography must be preferred: the example of Benin, West Africa, J. of African Earth Sci. 139, 341-353, https://doi.
- 411 org/10.1016/j.jafrearsci.2017.12.007
- 412 3. Aoulou K.A., Pistre S., Oga Y.M.S., Dewandel B., Lachassagne P. (2021). Improving the methods for processing
- 413 hard rock aquifers boreholes' databases. Application to the hydrodynamic characterization of metamorphic aquifers
- 414 from western Côte d'Ivoire. Water. 13, 3219. https://doi.org/10.3390/w13223219
- 415 4. Assemian E. A., Kouamé F. K., Saley M.B., Affian K., Youan Ta M., Jourda J.P.R., Biémi J. (2014). Étude de la
- 416 productivité d'un aquifère de socle et approche statistique pour la détermination des tranches de profondeurs
- 417 potentiellement productives : cas de la région de Bongouanou, Est de la Côte d'Ivoire. Revue des sciences de l'eau.
- 418 27 (1), 81-97.
- 419 5. Biémi J. (1992). Contribution à l'étude géologique, hydrogéologique et par télédétection des bassins versants sub-
- 420 sahéliens du socle précambrien d'Afrique de l'Ouest : hydrostructurale, hydrodynamique, hydrochimie et isotopie
- 421 des aquifères discontinus de sillons et aires granitiques de la haute Marahoué (Côte d'Ivoire). Thèse de Doctorat
- d'Etat ès Sciences Naturelles. Université de Cocody. Abidjan (Côte d'Ivoire). 493 p.
- 423 6. Bouatrin K. D., Kouame I. K., Douagui A. G., Kouassi K. A., Goula, B. T. A. (2022). Conceptual model of
- 424 aquifers in the bedrock zone of the marahoué watershed (Centre-West of Ivory Coast). J. of Geoscience and
- 425 Environment Protection. 10, 229-256. https://doi.org/10.4236/gep.2022.107014
- 426 7. Cho M. J., Choi Y.-S., Ha K.-C., Kee W.-S., Lachassagne P. and Wyns R. (2002). Paleoweathering covers in
- 427 Korean hard-rocks: a methodology for mapping their spatial distribution and the thickness of their constituting
- 428 horizons: application to identify brittle deformation and hard-rocks hydrogeology. Kigam Bull. 6, 12-25.
- 429 8. Courtois N., Lachassagne P., Wyns R., Blanchin R., Bougaïre F.D., Some S. and Tapsoba, A. (2010). Large-scale
- 430 mapping of hard-rock aquifer properties applied to Burkina Faso. Ground Water. 48, 269-283.
- 431 9. Delor C., Diaby I., Simeon Y., Yao B., Djama A., Okou A., Konaté S., Taslet J-P., Vidal M., Traoré I.,
- Dommanget A., Cautru J-P., Konan G. et Chiron J-C (1995). Carte Géologique de la Côte d'Ivoire à 1/200 000 ;
- 433 Feuille Grand-Lahou, Mémoire de la Direction des Mines et de la Géologie, n°5, Abidjan, Côte d'Ivoire
- 434 10. DesRoches, A., Danielescu, S., Butler, K., 2014. Structural controls on groundwater f low in a fractured bedrock
- 435 aquifer underlying an agricultural region of northwestern New Brunswick, Canada. Hydrogeol. J. 22, 1067–1086.
- 436 11. Dewandel B., Lachassagne P., Wyns R., Marechal, J.C. and Krishnamurthy N.S. (2006). A generalized 3-D
- 437 geological and hydrogeological conceptual model of granite aquifers controlled by single or multiphase weathering.
- 438 J. of Hydrol., 330, 260-284.
- 439 12. Dewandel B., Lachassagne P., Zaidi F. K., Chandra S. (2011). A conceptual hydrodynamic model of a
- 440 geological discontinuity in hard rock aquifers: Example of a quartz reef in granitic terrain in South India. J. of
- 441 Hydrol., 405, 474-487.

- 442 13. Douagui A. G., Kouadio S.K.A., Mangoua O. M., Kouassi A. K., Kouamé B.K., Savané I. (2019). Using specific
- 443 capacity for assessing of the factors controlling borehole productivity in crystalline bedrock aquifers of N'Zi, Iffou
- 444 and Moronou regions in the eastern area of Côte d'Ivoire, Groundwater for S. D.,
- 445 https://doi.org/10.1016/j.gsd.2019.100235
- 446 14. Géomines (1982). Inventaire hydrogéologique appliqué à l'hydraulique villageoise. Ministère des Travaux
- 447 Publics et des Transports, Direction Centrale de l'Hydraulique, République de Côte d'Ivoire, carte de Grand-Lahou.
- 448 26p.
- 449 15. Holland, M., Witthüser, K.T., 2011. Evaluation of geologic and geomorphologic influences on borehole
- 450 productivity in crystalline bedrock aquifers of Limpopo Province, South Africa. Hydrogeol. J., 22 (19), 1062-1083.
- 451 16. Kouame I. K., Douagui A. G., Bouatrin D. K., Kouadio S.K.A., Savané I. (2021). Assessing the hydrodynamic
- 452 properties of the fissured layer of granitoid aquifers in the Tchologo region (Northern Côte d'Ivoire), Helion,
- 453 https://doi.org/10.1016/j.heliyon.2021.e07620
- 454 17. Kouamé K.F. (1999). Hydrogéologie des aquifères discontinus de la région semi-montagneuse de Man-Danané
- 455 (Ouest de la Côte d'Ivoire). Apport des données des images satellitales et des méthodes statistique et fractale à
- 456 l'élaboration d'un système d'information hydrogéologique à référence spatiale. Thèse de Doctorat 3ème cycle.
- 457 Université Cocody. Abidjan (Côte d'Ivoire).
- 458 18. Lachassagne P., Ahmed S., Dewandel B., Courtois N., Maréchal J.C. Perrin J. and Wyns R. (2009). Recent
- 459 improvements in the conceptual model of hard rock aquifers and its application to the survey, management,
- 460 modeling and protection of groundwater. Groundwater and Climate in Africa (Proceedings of the Kampala
- 461 Conference, June 2008) IAHS Publ. no.334, pp 250-256.
- 462 19. Lachassagne P., Wyns R. and Dewandel B. (2011). The fracture permeability of Hard Rock Aquifers is due
- neither to tectonics, nor to unloading, but to weathering processes. Terra Nova, Vol. 23, pp 145-161.
- 464 20. Lachassagne, P., Dewandel B., Wyns R. (2015). Le modèle conceptuel hydrogéologique des aquifères de socle
- 465 altéré et ses applications pratiques, Colloque Aquifères de socle : le point sur les concepts et les applications
- opérationnelles, La Roche-sur-Yon, 11-13 juin 2015.
- 467 21. Lachassagne P., Dewandel B., Wyns R. (2021). Review: Hydrogeology of weathered crystalline/hard-rock
- 468 aquifers-Guidelines for the operational survey and management of their groundwater resources. Hydrogeol. J., 29,
- 469 34, https://doi.org/10.1007/s10040-021-02339-7.
- 470 22. Lasm T., 2000. Hydrogéologie des réservoirs fracturés de socle : analyses statistique et géostatistique de la
- 471 fracturation et des propriétés hydrauliques. Thèse unique. Univ. Poitiers (France). 233p.
- 472 23. Maréchal J-C., Wyns R., Lachassagne P., Subrahmanyam K. and Touchard F. (2003). Anisotropie verticale de la
- 473 perméabilité de l'horizon fissuré des aquifères de socle : concordance avec la structure géologique des profils
- d'altération. C. R. Géosciences, 335, 451-460.
- 475 24. Savané I. (1997). Contribution à l'étude géologique et hydrogéologique des aquifères discontinus du socle
- 476 cristallin d'Odienné (Nord-Ouest de la Côte d'Ivoire). Apport de la télédétection et d'un système d'information
- 477 géographique à référence spatiale. Thèse de Doctorat d'Etat ès Sciences Naturelles. Univ. Cocody (Côte d'Ivoire).
- 478 332 p
- 479 25. Tagnon B. O., Lasm T., Douagui A. G., Savane I. (2016). Statistical and geostatistical analysis of lineaments
- 480 network mapped in the precambrian basement: case of Divo-Oumé region (southern Côte d'Ivoire). European
- 481 Scientific Journal, 12 (33), 299-318.

- 482 26. Tagnon O.B., Assoma T.V., Mangoua O.M.J., Douagui G.A., Kouame, F.K., Savane I. (2018). Contribution of
- 483 SAR/RADARSAT-1 and ASAR/ ENVISAT images to geological structural mapping and assessment of lineaments
- density in Divo-Oumé area (Côte d'Ivoire). Egypt. J. Remote Sens. SpaceSci. 23 (2), 231-241.
- 485 27. Tagnon B.O., Oularé S., Kouamé K.I., Kouassi K.A., Kouadio Z.A., Savané I. (2020). Fully integrated and
- 486 physically-based approach for simulating water flows in a large-scale, heavily-agricultural and low-instrumented
- 487 watershed. J. of Hydrol., https://doi.org/10.1016/j.jhydrol.2020.124781
- 488 28. Tagnon B.O. (2021). Modélisation intégrée et à base physique des écoulements des eaux de surface et de
- 489 subsurface : application au bassin versant de la rivière Boubo, Sud de la Côte d'Ivoire. Thèse unique. Université
- 490 NanguiAbrogoua, Côte d'Ivoire, 242p.
- 491 29. Vouillamoz J. M., Lawson F. M. A., Yalo N., Descloitres M. (2014). The use of magnetic resonance sounding
- 492 for quantifying specific yield and transmissivity in hard rock aquifers: the example of Benin. J Appl Geophys 107,
- 493 16-24. https://doi.org/10.1016/j.jappgeo.2014.05.012
- 494 30. Walraevens K., Bennett G., Alfarrah N., Gebreyohannes T., Berhane G., Hagos M., Hussien A., Nigate F., Belay
- 495 A.S., Birhanu A., Yenehun A. (2025). Assessing the potential of volcanic and sedimentary rock aquifers in Africa:
- 496 emphasizing transmissivity, water quality, and recharge as key evaluation metrics. Water, 17, 109. https://
- 497 doi.org/10.3390/w17010109
- 498 31. Wyns R., Baltassat J.M., Lachassagne P., Legtchenko A. and Vairon J. (2004). Application of proton magnetic
- 499 resonance soundings to groundwater reserves mapping in weathered basement rocks (Brittany, France). Bull. Soc.
- 500 Géol. Fr., Vol. 175, pp 21 34.

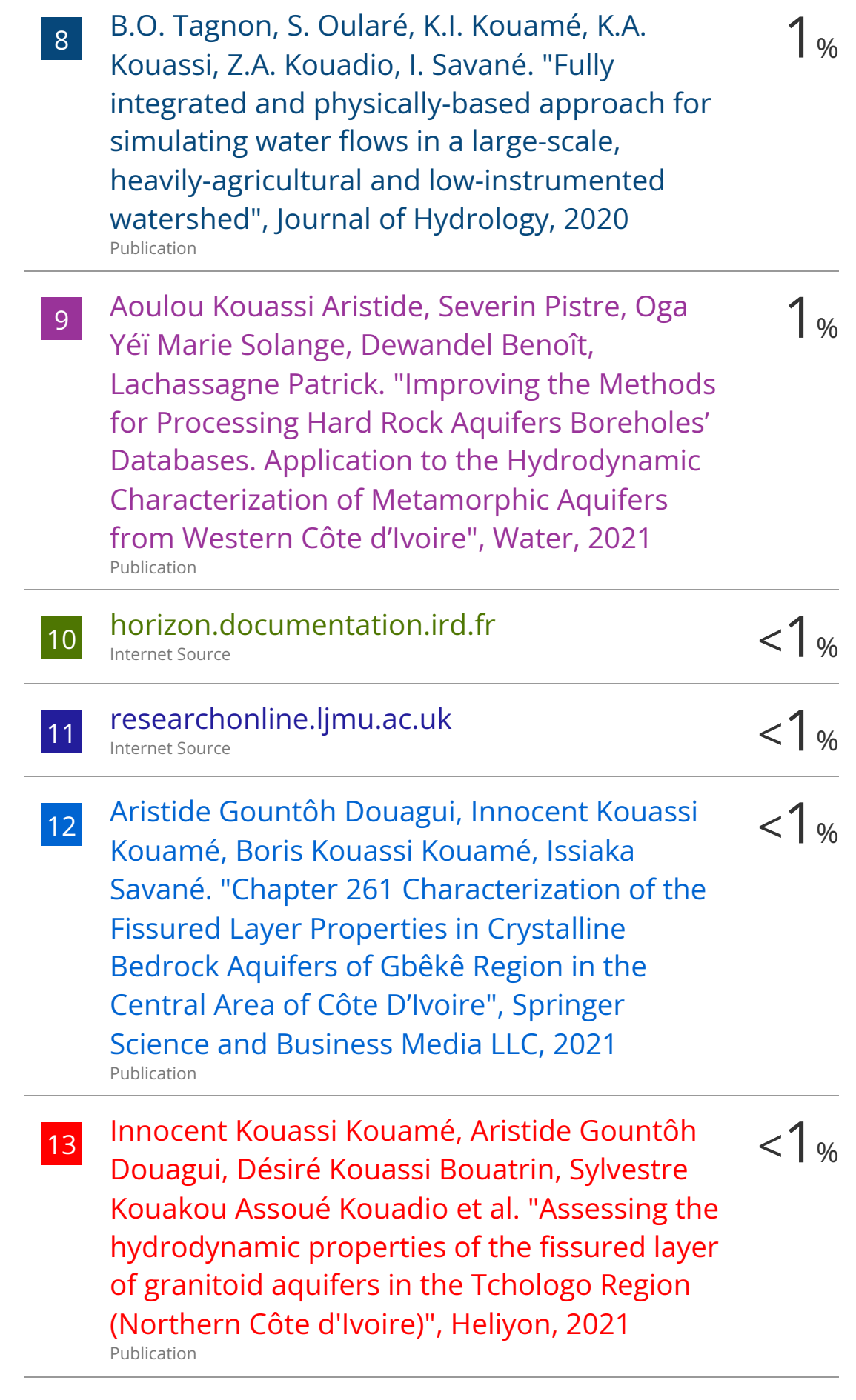
Acknowledgement

The authors thank the anonymous reviewers whose valuable contributions greatly improved the manuscript.

503 504

HARD ROCKS AQUIFER PROPERTIES ESTIMATION AND MAPPING THE OPTIMAL DEPTH OF WELLS TO DRILL IN DIVOGUITRY AREA, SOUTHERN CÃ TE DÂ IVOIRE

Bouagui, Desire Kouassi Bouatrin, Sylvestre Kouakou Assoué Kouadio et al. "Assessing the hydrodynamic properties of the fissured layer of granitoid aquifers in the Tchologo Region (Northern Côte d'Ivoire)", Heliyon, 2021 Publication 2 www.mdpi.com Internet Source 1 Rock Armand Michel Bouadou, Kouamé Auguste Kouassi, Adama Coulibaly, Gountôh Aristide Douagui, Théophile Gnagne. "Mapping of Productive Aquifer Horizons in the Crystalline Bedrock Environment of the Bounkani Region (Northeastern Ivory Coast)", Open Journal of Geology, 2025 Publication 1 Iink.springer.com Internet Source 1 1		LITY REPORT	A IL DA IVOIRL	
1 Innocent Kouassi Kouame, Aristide Gountôh Douagui, Désiré Kouassi Bouatrin, Sylvestre Kouakou Assoué Kouadio et al. "Assessing the hydrodynamic properties of the fissured layer of granitoid aquifers in the Tchologo Region (Northern Côte d'Ivoire)", Heliyon, 2021 Publication 2 www.mdpi.com	SIMILA			
Douagui, Désiré Kouassi Bouatrin, Sylvestre Kouakou Assoué Kouadio et al. "Assessing the hydrodynamic properties of the fissured layer of granitoid aquifers in the Tchologo Region (Northern Côte d'Ivoire)", Heliyon, 2021 Publication 2	PRIMAR	Y SOURCES		
 coek.info	1	Douagui, Désiré Kouas Kouakou Assoué Koua hydrodynamic proper of granitoid aquifers in (Northern Côte d'Ivoir	ssi Bouatrin, Sylvadio et al. "Asses ties of the fissur n the Tchologo F	vestre ssing the ed layer Region
Rock Armand Michel Bouadou, Kouamé Auguste Kouassi, Adama Coulibaly, Gountôh Aristide Douagui, Théophile Gnagne. "Mapping of Productive Aquifer Horizons in the Crystalline Bedrock Environment of the Bounkani Region (Northeastern Ivory Coast)", Open Journal of Geology, 2025 Publication www.journalijar.com Internet Source 1	2	• • • • • • • • • • • • • • • • • • •		1%
Auguste Kouassi, Adama Coulibaly, Gountôh Aristide Douagui, Théophile Gnagne. "Mapping of Productive Aquifer Horizons in the Crystalline Bedrock Environment of the Bounkani Region (Northeastern Ivory Coast)", Open Journal of Geology, 2025 Publication www.journalijar.com Internet Source 1	3			1%
link.springer.com Internet Source 1	4	Auguste Kouassi, Adar Aristide Douagui, Théo "Mapping of Productive the Crystalline Bedroo Bounkani Region (Nor Open Journal of Geolo	ma Coulibaly, Go ophile Gnagne. ve Aquifer Horizo k Environment o theastern Ivory	ountôh ons in of the
Internet Source	5			1%
www.researchgate.net	6	. •		1 %
Internet Source	7	www.researchgate.ne	t	1%



"Geology and geochronology of the Archean plutonic rocks in the northeast Democratic Republic of Congo", Precambrian Research, 2021

Publication

H. Nouradine, C. Schamper, D. Valdes, I. 19 Moussa, D. Ramel, V. Plagnes. "Integração de dados geológicos, hidrogeológicos e geofísicos para identificar recursos hídricos subterrâneos em áreas de embasamento granítico (Maciço Guéra, Chade)", Hydrogeology Journal, 2024

<1%

Mozimwè ANI, Jessy JAUNAT, Béatrice MARIN, <1% 20 Frederic HUNEAU, Kissao GNANDI. "Using archive hydrogeological data to enhance the hydrodynamic knowledge of hardrock aquifers in Western Africa", Journal of African Earth Sciences, 2024 Publication repository.stiki.ac.id 21 Internet Source Jean-Christophe Comte, Rachel Cassidy, Janka 22 Nitsche, Ulrich Ofterdinger, Katarina Pilatova, Raymond Flynn. "A tipologia de aquíferos irlandeses de rochas duras baseada numa aproximação hidrogeológica e geofísica integrada", Hydrogeology Journal, 2012 Publication onlinelibrary.wiley.com 23 Internet Source www.spiedigitallibrary.org 24 Internet Source jistee.org 25 Internet Source Bertrand Houngnigbo Akokponhoue, Marc 26 Youan Ta, Abdoukarim Alassane, Nesny Yanovoh Akokponhoue, Nicaise Yalo. "Chapter 1 Contribution of Remote Sensing and GIS to the Mapping of Fractured Reservoirs in the Donga Department (Northwestern Benin) for a Sustainable Management of Their Resources", Springer

Publication

Science and Business Media LLC, 2024

28	bec.uac.bj Internet Source	<1%
29	journals.pan.pl Internet Source	<1%
30	Abdou Raouf, Xiaohui Lu, Kasi Njeudjang, Mohamed Koulibaly, Nga Essomba Tsoungui Philomène Estelle. "Quasi-3D modeling of vertical electrical sounding for mapping hard rock aquifers in the Adamawa Yadé Domain, Central Africa", Journal of African Earth Sciences, 2025 Publication	<1%
31	Albert Asare, Emmanuel K. Appiah-Adjei, Frederick Owusu-Nimo, Bukari Ali. "Lateral and vertical mapping of salinity along the coast of Ghana using Electrical Resistivity Tomography: the case of Central Region", Results in Geophysical Sciences, 2022	<1%
32	Ayraud, V "Compartmentalization of physical and chemical properties in hard-rock aquifers deduced from chemical and groundwater age analyses", Applied Geochemistry, 200809	<1%
33	Engineering Geology for Society and Territory - Volume 3, 2015. Publication	<1%
34	Razack, M, M Ta, and T Lasm. "Geostatistical assessment of the transmissivity of crystalline fissured aquifer in the Bondoukou region, north-eastern Cote d,Äôlvoire", IAH - Selected Papers on Hydrogeology, 2008.	<1%

35	Z. Mfonka, P.S. Kouassy Kaledje, A. Anaba Onana, D. Nsangou, A. Kpoumie, M. Zammouri, P-D. Ndjigui, J.R. Ndam Ngoupayou. "Integrated geophysical and remote sensing/GIS interpretation for delineating the structural elements and groundwater aquifers of the Foumban locality, Western Highlands of Cameroon (WHC)", Geosystems and Geoenvironment, 2025 Publication	<1%
36	discovery.ucl.ac.uk Internet Source	<1%
37	docslide.us Internet Source	<1%
38	pubs.sciepub.com Internet Source	<1%
39	www.aquanty.com Internet Source	<1%
40	Bertrand Ouessé Tagnon, Vincent Tchimou Assoma, Jules Mangoua Oi Mangoua, Aristide Gountôh Douagui et al. "Contribution of SAR/RADARSAT-1 and ASAR/ENVISAT images to geological structural mapping and assessment of lineaments density in Divo- Oume area (Côte d'Ivoire)", The Egyptian Journal of Remote Sensing and Space Science, 2018 Publication	<1%
41	Nathalie Courtois. "Large-Scale Mapping of Hard-Rock Aquifer Properties Applied to Burkina Faso", Ground Water, 03/2010	<1%

